Developmental Biology 364 (2012) 178–191

Contents lists available at SciVerse ScienceDirect

Developmental Biology

journal homepage: www.elsevier.com/developmentalbiology

N-cadherin and β1-integrins cooperate during the development of the enteric nervous system

Florence Broders-Bondon [a], Perrine Paul-Gilloteaux [a,b], Camille Carlier [a], Glenn L. Radice [c], Sylvie Dufour [a,*]

[a] Institut Curie/CNRS UMR144, Paris, France
[b] Cell and Tissue Imaging Facility, PICT-IBiSA, Paris, France
[c] Thomas Jefferson University, Center for Translational Medicine, Department of Medicine, Philadelphia, PA 19107, USA

ARTICLE INFO

Article history:
Received for publication 10 November 2011
Revised 18 January 2012
Accepted 2 February 2012
Available online 10 February 2012

Keywords:
Enteric nervous system
Neural crest cells
Migration
N-cadherin
β1-integrins
Cross-talk

ABSTRACT

Cell adhesion controls various embryonic morphogenetic processes, including the development of the enteric nervous system (ENS). Ablation of β1-integrin (β1−/−) expression in enteric neural crest cells (ENCC) in mice leads to major alterations in the ENS structure caused by reduced migration and increased aggregation properties of ENCC during gut colonization, which gives rise to a Hirschsprung's disease-like phenotype.
In the present study, we examined the role of N-cadherin in ENS development and the interplay with β1 integrins during this process. The Ht–PA–Cre mouse model was used to target gene disruption of N-cadherin and β1 integrin in migratory NCC and to produce single- and double-conditional mutants for these two types of adhesion receptors.
Double mutation of N-cadherin and β1 integrin led to embryonic lethality with severe defects in ENS development. N-cadherin-null (Ncad−/−) ENCC exhibited a delayed colonization in the developing gut at E12.5, although this was to a lesser extent than in β1−/− mutants. This delay of Ncad−/− ENCC migration was recovered at later stages of development. The double Ncad−/−; β1−/− mutant ENCC failed to colonize the distal part of the gut and there was more severe aganglionosis in the proximal hindgut than in the single mutants for N-cadherin or β1-integrin. This was due to an altered speed of locomotion and directionality in the gut wall. The abnormal aggregation defect of ENCC and the disorganized ganglia network in the β1−/− mutant was not observed in the double mutant. This indicates that N-cadherin enhances the effect of the β1−integrin mutation and demonstrates cooperation between these two adhesion receptors during ENS ontogenesis.
In conclusion, our data reveal that N-cadherin is not essential for ENS development but it does modulate the modes of ENCC migration and acts in concert with β1−integrin to control the proper development of the ENS.

Introduction

The enteric nervous system (ENS) is part of the peripheral nervous system that controls gastrointestinal tract function. The ENS is derived from migratory vagal neural crest cells (NCC) that arise from the neural tube at the level of somites 1–7 as well as a small proportion of NCC from the posterior sacral region (Heanue and Pachnis, 2007; Young et al., 2004a). Vagal NCC enter the foregut rostrally at E9–9.5 and are termed enteric neural crest cells (ENCC). They then colonize the entire gastrointestinal tract by migrating in the gut wall in a rostro-caudal direction through the midgut, the caecum, and the hindgut; the process is completed by E14.5. During colonization, ENCC actively proliferate and migrate using complex patterns of cell movements. Chains of ENCC are observed in the linear portions of the midgut and hindgut whereas more isolated ENCC are found in the caecum where they adopt a mesenchymal mode of migration and pause for several hours (Barlow et al., 2008; Druckenbrod and Epstein, 2005; Young et al., 2004b).

Defects in ENCC migration result in an absence of enteric ganglia in the terminal region of the gut. This leads to intestinal obstruction and dramatic distension of the distal bowel described in humans as Hirschsprung's disease (HSCR: congenital aganglionosis) or megacolon (Heanue and Pachnis, 2007; Jiang et al., 2011). These conditions arise in 1/6670 live births among Europeans, 1/3570 live births among Asians, and 1/4760 live births among Africans (Jiang et al., 2011). HSCR is sporadic for most patients, although some cases are familial with a non-Mendelian inheritance, which suggests that there are multifactorial causes. Mouse studies have identified genetic factors leading to HSCR-like phenotypes (Heanue and Pachnis, 2007). Genes associated with HSCR include those encoding GDNF and its receptors GFRα1 and Ret, endothelin-3 (EDN3) and its G-protein-coupled receptor EDNRB, and the transcription factors Sox10 and Zeb2 (Amiel et al., 2008). However, mutations in these HSCR-associated genes account for less than 50% of familial cases of HSCR and only for a small proportion of sporadic cases. This suggests that

* Corresponding author at: Institut Curie, Section Recherche, UMR144, 26 rue d'Ulm, 75248 Paris Cedex 05, France. Fax: +33 156246319.
E-mail address: sylvie.dufour@curie.fr (S. Dufour).

0012-1606/$ – see front matter © 2012 Elsevier Inc. All rights reserved.
doi:10.1016/j.ydbio.2012.02.001

the incomplete penetrance of HSCR is due to interactions between HSCR and modifier genes (Parisi and Kapur, 2000).

Alterations in gut colonization by ENCC, the mode of ENCC migration, and the organization of the ganglia network can also reflect variation in the molecular mechanisms driving ENCC interactions and their progression in response to their environment. During ENS development, several extracellular matrix (ECM) components, factors, and cell types are present in the gut wall. ENCC express a large repertoire of adhesion receptors which control their adhesion to ECM and neighboring cells (reviewed in (Breau and Dufour, 2009)).

ENCC express the neural cell-adhesion molecule (NCAM), as well as its polysialylated forms PSA-NCAM and L1-CAM. PSA-N-CAM is required for remodeling chains of neurons into mature patterns of ganglia and connectives of the enteric plexuses; this process is regulated by BMP-4 (Faure et al., 2007). L1-CAM is required for chain migration of NCC in the developing gut because disruption of L1 activity slows NCC migration and increases the number of solitary NCC (Anderson et al., 2006). Recently, L1-CAM has been identified as a modifier gene for the *SOX10* phenotype during ENS development (Wallace et al., 2010).

ENCC also express cadherins, which are cell–cell adhesion molecules that mediate Ca^{2+}-dependent homophilic adhesion. Cadherins play a crucial role during the formation of tissues and neural networks, and in maintaining cellular cohesivity during development and morphogenesis (reviewed in (Gumbiner, 2005)). ENCC mostly express N-cadherin, and lower levels of cadherin-6 and cadherin-11 (Breau et al., 2006; Gaidar et al., 1998). Inactivation of N-cadherin in the central nervous system revealed its crucial role in NCC delamination (Bronner-Fraser et al., 1992; Nakagawa and Takeichi, 1998) and migration during chick development (Kasemeier-Kulesa et al., 2006). Ablation of N-cadherin with Wnt1–Cre resulted in embryonic lethality by E13 associated with severe cardiovascular defects (Luo et al., 2006). This prevented analysis of N-cadherin function in ENCC ontogeny and to date, the role of cadherins during ENCC colonization has not been investigated.

ENCC express a repertoire of integrins including α4β1, α5β1, α6β1, αVβ1, αVβ3, and αVβ3 (Breau et al., 2009; Iwashita et al., 2003; Kruger et al., 2003). Integrins are the main receptors for the ECM (Campbell and Humphries, 2011; Hynes, 2002) and, in cooperation with receptors for growth factors and cytokines, regulate cell adhesion, migration, proliferation, survival, and differentiation. It has been previously shown that integrins and cadherins coordinate trunk NCC migration in vitro. In this process, β1-integrin and β3-integrin are at the origin of a signaling cascade which controls the distribution and activity of N-cadherin (Monier-Gavelle and Duband, 1997). β1-integrin depletion in ENCC severely affects ENS organization by increasing cell aggregation through a calcium-dependent mechanism involving cadherins (Breau et al., 2006). We have previously reported that mice lacking β1-integrin in the neural crest lineage exhibit a HSCR-like phenotype characterized by aganglionosis in the descending colon (Breau et al., 2006). ENCC lacking β1-integrin stop migration before they reach the caecum and hindgut (Breau et al., 2009); they become abnormally aggregated in the gut wall by Ca^{2+}-dependent mechanisms, suggesting that cadherins were implicated in their formation.

The present study analyzes the effects of conditional inactivation of N-cadherin and the double inactivation of N-cadherin and β1-integrin in ENCC to determine their functions and interplay during ENS formation. We showed that depletion of N-cadherin in ENCC altered their migratory properties, which caused a transient delay of ENCC progression during gut colonization. However, we observed a more severe ENS phenotype in double mutants for N-cadherin and β1-integrin with extended aganglionosis of the colon compared with single mutants. Analysis of the colonized part of the gut from double mutants revealed a partial rescue of the ganglia network organization compared with β1-integrin mutants indicating that N-cadherin and β1 integrins cooperate during ENS development.

Material and methods

Mouse maintenance and genotyping

$Ncad^{fl/fl}$ mice (Kostetskii et al., 2005) were crossed with $\beta1^{fl/fl}$; $YFP^{fl/fl}$ mice (Breau et al., 2009; Potocnik et al., 2000; Srinivas et al., 2001) to produce triple homozygous $Ncad^{fl/fl}$;$\beta1^{fl/fl}$;$YFP^{fl/fl}$ animals. Homozygous Ht–PA–Cre mice (Ht–PA–Cre:Ht–PA–Cre) described in (Pietri et al., 2003) were crossed with mice heterozygous for N-cadherin-null allele ($Ncad^{neo/wt}$; (Radice et al., 1997)) to generate homozygous Ht–PA–Cre;$Ncad^{neo/wt}$ breeder males.

The genetic backgrounds of the mice were: Ht–PA–Cre, B6/D2/C57; $Ncad^{fl/fl}$,129 Sv/C57; and $\beta1^{fl/fl}$, 129 Sv/C57.

For single N-cadherin mutant analysis, Ht–PA–Cre;$Ncad^{neo/wt}$ males were crossed with $Ncad^{fl/fl}$;$\beta1^{fl/fl}$;$YFP^{fl/fl}$ females to produce Ht–PA–Cre;$Ncad^{\mathbf{neo/fl}}$;$\beta1^{wt/fl}$;$YFP^{wt/fl}$ mice (referred to as Ncad mutants), and Ht–PA–Cre;$Ncad^{\mathbf{wt/fl}}$;$\beta1^{wt/fl}$;$YFP^{wt/fl}$ mice (referred to as controls).

For double-mutant analysis, we crossed Ht–PA–Cre;$Ncad^{neo/wt}$ animals with Ht–PA–Cre;$\beta1^{neo/wt}$ animals (Pietri et al., 2004) to obtain Ht–PA–Cre/Ht–PA–Cre;$Ncad^{neo/wt}$;$\beta1^{neo/wt}$ breeder males. These were crossed with $Ncad^{fl/fl}$;$\beta1^{fl/fl}$;$YFP^{fl/fl}$ females. Four genotypes were obtained in the progeny: Ht–PA–Cre;$Ncad^{\mathbf{neo/fl}}$;$\beta1^{\mathbf{neo/fl}}$;$YFP^{wt/fl}$ (referred to as double Ncad- and β1-mutants [DM]), Ht–PA–Cre;$Ncad^{\mathbf{neo/fl}}$;$\beta1^{\mathbf{wt/fl}}$;$YFP^{wt/fl}$ (referred to as N-cad mutants [Ncad−/− or Ncad mutant]), Ht–PA–Cre;$Ncad^{\mathbf{wt/fl}}$;$\beta1^{\mathbf{neo/fl}}$;$YFP^{wt/fl}$ (referred to as β1-integrin mutant [β1−/− or β1 mutant]), and Ht–PA–Cre;$Ncad^{\mathbf{wt/fl}}$;$\beta1^{\mathbf{wt/fl}}$;$YFP^{wt/fl}$ (referred to as controls). ENCC from Ncad mutants were named Ncad-null and ENCC from β1-mutants were named β1-null.

Experiments were performed in accordance with the ethical guidelines of the French National Center for Scientific Research (CNRS). Genotyping was performed using primers synthesized by Eurogentec (Belgium); the β1 primers for Ht–PA–Cre and β1-integrin mice have been described in Pietri et al. (2004). The sense and antisense primers used for N-cadherin neo amplification were: 5′-GGCCGAATGATTTTAG-GATTTG-3′, and 5′-TTCTCGTGCTTTACGGTATC-3′.

Immunostainings and organotypic cultures

Immunostaining on paraffin sections was performed as previously described in Pietri et al. (2004) using the antibodies listed in Table S1 in the Supplementary materials section. β-catenin immunostaining was performed as described in Fre et al. (2009). TUJ1 whole-mount immunostaining was carried out as described in Stanchina et al. (2006). Ex-vivo cultures of guts, 2D-cultures of E12.5 midgut rings, and gut dissociation assays were carried out as described in Breau et al. (2009).

Video time-lapse imaging and confocal microscopy

Imaging was performed at the Nikon Imaging Centre at the Institut Curie-CNRS (NIMCE@IC-CNRS). Video-time lapses of gut ex-vivo cultures were carried out as described previously (Breau et al., 2009) using a Nikon Eclipse Ti inverted video-microscope equipped with a cool CDD-camera in a humid atmosphere of 5% CO_2 kept at 37 °C. Whole-mount TUJ1 immunostained guts were analyzed with an inverted confocal A1-R Nikon microscope. Three 3D stacks were acquired at the proximal, median, and distal midgut (called Mg1, Mg2 and Mg3, respectively) and the proximal, median, and distal hindgut (called Hg1, Hg2, and Hg3, respectively) for the control and mutant mice, respectively, and for two distinct offsprings. These are respectively referred to as confocal dataset A and confocal dataset B in the results section.

Image analysis

Individual ENCC of ex-vivo gut cultures were tracked manually using Metamorph 7.7.3.0 software to determine their speed of locomotion.

To quantify the ENCC density within the gut tissue, we analyzed the area of the spaces devoided of YFP$^+$ cells (ENCC). Segmentation was applied on the maximum intensity projection of the confocal slices taken from stained guts, using a self-developed imageJ macro based on K-means clustering (Dima et al., 2011). K-means is a least-squares partitioning method of the intensity histogram of an image into K groups. For the segmentation we used K=3 groups. Free space between YFP$^+$ ENCC was identified as the cluster with the lowest mean intensity (see Supplementary data, Fig. S2). The average area of all non-connected background clusters was measured in pixel squares, as all images have the same calibration.

To quantitatively compare the aspect of the ENS network in different conditions, we analyzed the texture of the TUJ1$^+$ networks, a gray-level-co-occurrence matrix (GLCM) with pixel offsets of 10 and two perpendicular directions was used to calculate the Haralick textural feature groups as described in Muldoon et al. (2010). This analysis compares the distribution and clustering of pixels and not only the intensities. The five GLCM criteria used were angular second moment (ASM; similarity and entropy), contrast, correlation, and inverse different moment (IDM; homogeneity). Entropy and similarity do not depend of pixel intensity. Entropy is a measure about how organized is the network and measures randomness of patterns. Similarity measures how often a pair of neighbors occurs and then measures homogeneity as well. Contrast gives the information about how much different is the pair pixel intensity (in 2 directions in our study). A uniform image will have no contrast, while a checkerboard image will get a higher contrast. Correlation (here for the GLCM correlation) measures the linear dependency between pixel intensity and the one of its neighbors and will augment in the presence of patterns, it is linked to both clustering and intensity of pixels. Homogeneity (Inverse Different Moment) is also based on pixel intensity, but in the reverse way from contrast and is less sensible to intensity variations. GLCM criteria were computed through a self-developed imageJ macro based on an Image J plugin http://rsbweb.nih.gov/ij/plugins/texture.html. Principal component analysis (PCA) was used which consists in creating a space where axes are linear combinations of the 5 GLCM criteria. These axes were computed such that the dispersion of all data was maximized. Five axes were created but only 2 in our case were sufficient to represent the dispersion of all data. This allowed us to work in a 2D space rather than in a 5D space with the same results without losing information. In this 2D space, the nearest two points are, the more similar they are. For PCA, three slices per 3D image of the confocal dataset were used as samples. PCA was performed using Matlab, Mathsworks. Each mutant phenotype was compared to that of the control and statistical analysis was performed using Student's *t* test. P values ranged from 10^{-4} to 10^{-5} and were defined as follows: >0.05: not significant (ns); 0.01–0.05: significant; 0.001–0.01: very significant; <0.01: extremely significant, as described in www.graphpad.com.

Results

The aim of the study was to investigate the effects of the conditional deletion of the N-cadherin gene during ENCC migration both in a wild-type context and a β1-integrin-null context for ENCC. Complete knock-out of the N-cadherin gene has been reported to be lethal at E10.0 due to heart-tube defects, whereas heterozygous animals are normal and fertile (Radice et al., 1997). For this reason, we used the previously described Ht–PA–Cre mice (Breau et al., 2009; Pietri et al., 2003, 2004) to specifically disrupt the N-cadherin gene, the β1-integrin gene, or both in mice ENCC without affecting the central nervous system.

To verify the loss of N-cadherin and β1-integrin proteins in the mutants, we performed immunostainings on paraffin sections of midgut at E12.5 (Fig. S1). Our results show: i) loss of N-cadherin expression for Ncad−/− ENCC (Fig. S1F,H) and DM (Fig. S1N,P); and ii) loss of β1-integrin expression in β1−/− ENCC (Fig. S1K,L) and DM (Fig. S1O,P). These conditional Cre/lox deletion systems therefore allow the efficient single and double removal of N-cadherin and β1-integrin in ENCC.

Defective neuronal colonization of the gut by N-cadherin and double-mutant ENCC

The distribution of enteric neurons reflects the progress of their migration during colonization of the gut. We therefore performed whole-mount immunofluorescence staining with the TUJ1 antibody to visualize the neuronal network in the guts of each class of genotyped embryos at different stages of development (see Figs. 1 and 2).

At E12.0, we observed a delay in migration for Ncad−/−, β1−/− and DM ENCC versus controls for all of the mutant embryos tested. The colonization front of TUJ1 positive staining was localized at the proximal hindgut in controls (Fig. 1A, white arrow; n=3), at the caecum in Ncad−/− embryos (Fig. 1B, white arrowhead; n=3), and at the distal midgut in DM (Fig. 1D, white arrowhead; n=4). Consistent with previous reports (Breau et al., 2006), the colonization front was located at entrance of the caecum in β1−/− embryos (Fig. 1C; white arrowhead; n=6).

At E13.5, the colonization front was localized in the middle of hindgut in controls (Fig. 1E; white arrow; n=7). For Ncad mutants, one of the three guts analyzed had a colonization front that was in a similar position to the controls, whereas the two others showed a slightly delayed upstream location (Fig. 1F, white arrowheads; n=3). The colonization front was located before the caecum in the DM (Fig. 1H, white arrowhead; n=2), and at the entrance of the hindgut in the β1−/− mutants (Fig. 1G; white arrowhead; n=5).

At E14.5, the colonization of the gut was complete in the controls (Fig. 2D4; white arrow; n=9) and almost complete in the Ncad mutants (Fig. 2C4; white arrowhead; n=7). In contrast, gut colonization had not reached the terminal part of the colon in the other mutants (Fig. 2; A4, B4, C4). TUJ1 staining stopped at the first half of the colon in the DM (Fig. 2A4; white arrowhead; n=4) but reached at least the central part of the colon in the β1−/− mutants (Fig. 2B4; n=8). In the colonized part of the guts, we observed no significant difference in the intensity of TUJ1 staining between the controls and mutants (Figs. 1 and 2), with similar numbers of TUJ1-positive cells.

At later stages (E18.5), there was still a lack of distal-gut colonization for DM and β1−/−, whereas Ncad−/− and controls exhibited similar phenotypes (data not shown).

These results demonstrate that there was a significant delay of neuronal colonization for single and double mutants compared with controls at E12 and E13.5. However, at later stages of ENS development, ENCC had entirely colonized the gut of the Ncad mutants. There is therefore a gradual increase in severity of the ENS phenotype which is slight and transient in Ncad−/−, severe in β1−/− and aggravated in DM, respectively.

The migration front was analyzed to compare the position of neuronal processes and YFP$^+$ ENCC at E14.5 by confocal microscopy (Fig. 3). As for neuronal colonization we observed that YFP$^+$ ENCC are retarded in β1−/− and DM mutants compared to Ncad−/− and controls. ENCC at the wave front were closely associated with the neurites (TUJ1$^+$ processes) in the Hg3 portion (white arrows) for control (Fig. 3A, B, C; n=3) and Ncad−/− (Fig. 3D, E, F; n=4). For the DM, similar interactions were observed in the Hg2 region, with neurites visibly associated with a few ENCC at the front (Fig. 3J, K, L; white arrows; n=4). In contrast, in β1−/− mutants we observed long neurites located ahead of the YFP$^+$ ENCC migratory front (white arrowheads; Fig. 3G, H, I) in the Hg2 region (n=5). Our results also indicated that adhesion between ENCC and axons was retained in DM at E14.5.

The neuronal organization of the midgut region of TUJ1 immunostained guts at E14.5 was further analyzed. Compilations of images

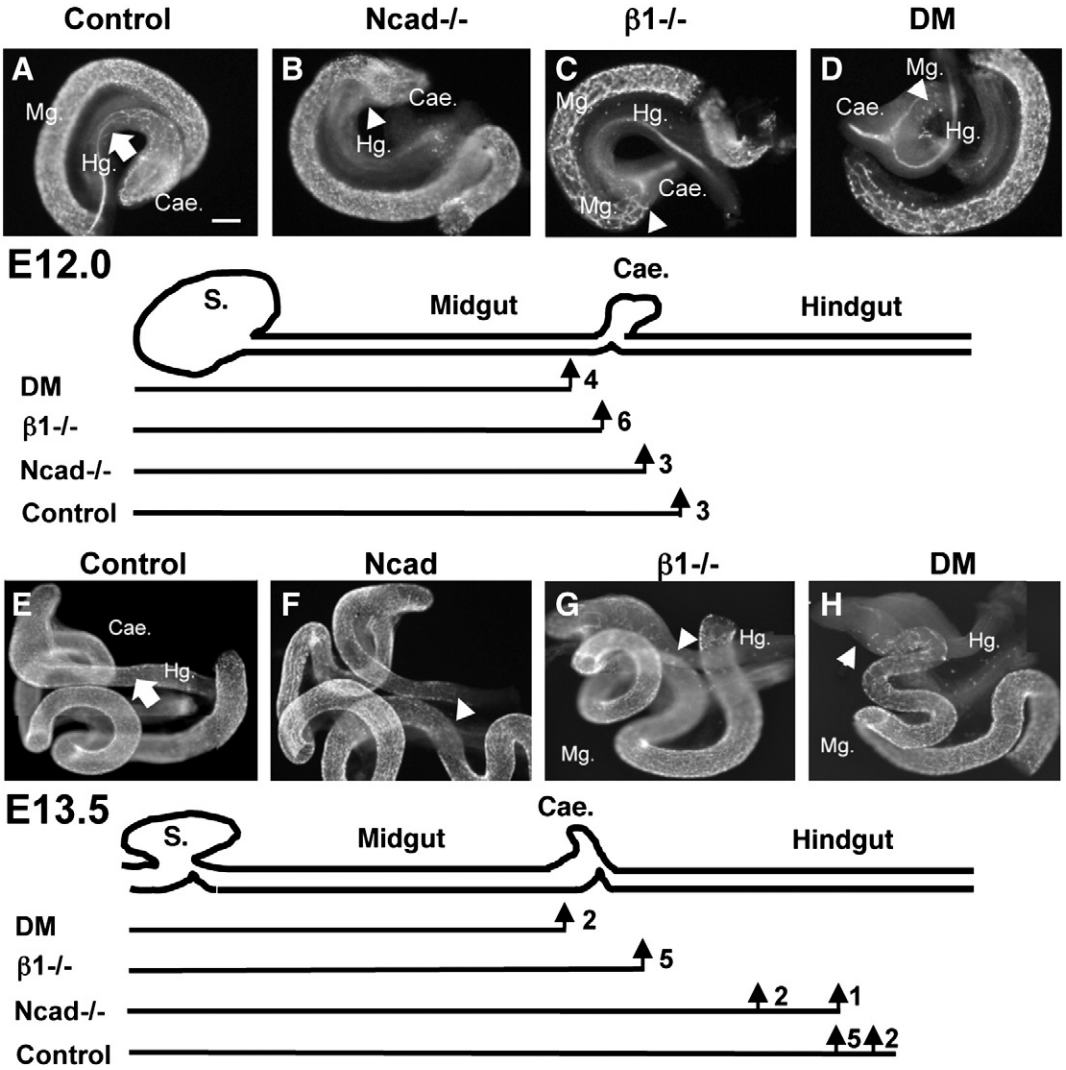

Fig. 1. Rostro-caudal neuronal colonization along the gastrointestinal tract of control and mutant mice at different stages of early development (E11.5–E13.5). Whole-mount immunofluorescent staining with the TUJ1 antibody (anti-β3 tubulin) to visualize the neuronal network and schematic representation of the stomach, midgut, caecum, and hindgut regions of the gut. Below the schemes, lines and perpendicular arrows indicate the extent of gut colonization for each class of genotyped embryos. The numbers of embryos with a defined defect is indicated on the right of each arrow. The TUJ1 staining pictures represent one example among the others mentioned on the drawing. At E12.0, there is a delay of migration for single (B, C) and double-mutants (D) compared with controls (A). Arrows indicate the position of the migratory front in controls; arrowheads indicate the position of the migratory front in mutants. The migratory front is located before the caecum for the double mutants (D). At E13.5, the migratory front is still located before the caecum for the double mutants (H) whereas it is localized in the proximal hindgut for Ncad mutants (F), β1 mutants (G), and controls (E). Midgut, caecum and hindgut are indicated as follows: Mg, Cae and Hg respectively. Scale bar = 150 μm.

from more than 10 independent experiments gave additional information and highlighted the disorganization of neuronal network for single and double mutants (Fig. 4B, C, D) compared with controls (Fig. 4A). At higher magnification, we observed that the neurites were less fasciculated in Ncad−/− (Fig. 4B). β1−/− mutants exhibited enlarged neuron-free regions and bigger neuron aggregates (white arrows). In DM, a rescue of the network organization was observed compared with β1−/− (Fig. 4D), and which was characterized by a decrease of the size of neurite-free spaces and aggregates

Comparative analysis of the neuronal network organization in gut organotypic cultures

To analyze the effects of these mutations on neuritogenesis in vitro, we carried out cultures of gut explants using rings of E13.5 midgut plated onto 2D substrata in 15 independent experiments. Vitronectin (VN) and fibronectin (FN) were used to produce a permissive substratum of adhesion and migration for the four ENCC genotypes, including β1−/− (Breau et al., 2009). After 24 h of culture, explants were stained with specific markers for Sox10+ (progenitors), HuD+ (neurons), and B-FABP+ (glial cells). To get a better view of the morphology of whole explants, images were first taken at low magnification (Fig. 4E–H, black pictures) that allows visualization of the neuronal network, delimited by blue dot-lines.

In control and Ncad−/− cultures, neurons formed a scattered network around the explants and outside the outgrowth of migratory mesenchymal cells (Fig. 4E, F). In contrast, only a few β1-null neurons were found located at the periphery of the explants (Fig. 4G, black arrows). The DM displayed a similar distribution to that observed for control and Ncad−/−.

The ENCC shown in white boxes at lower magnification in Fig. 4E–H correspond to the higher magnification images in Fig. 4I–L. The control neurons and their neurites formed a scattered network on substrata (Fig. 4I). The Ncad−/− neurons were scattered with long and thick neuronal processes (Fig. 4J, N arrows). By contrast, the β1−/− neurons were organized into highly cohesive aggregates that did not adhere to the surface (Fig. 4K, black arrow), as previously described by Breau et al. (2006). Although we did not observe any aggregates in DM in

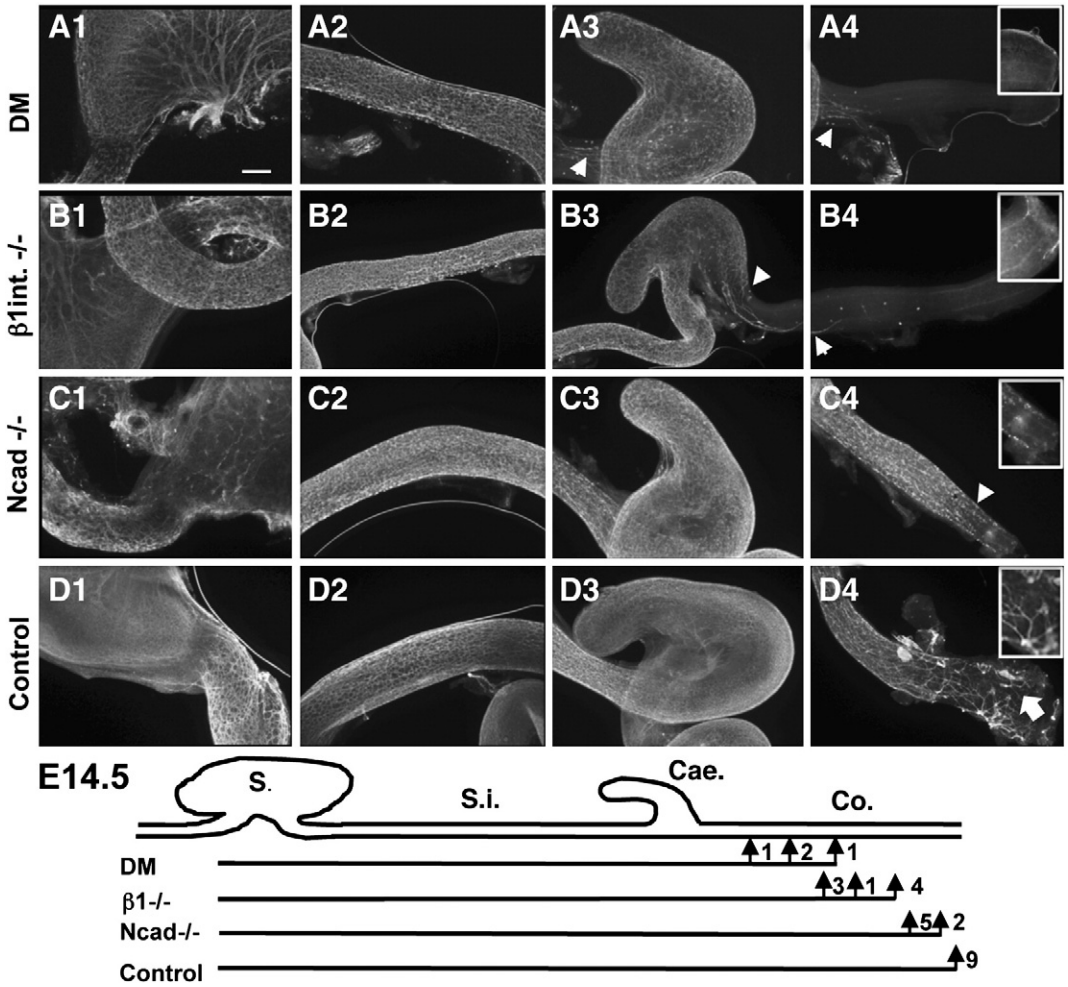

Fig. 2. Rostro-caudal neuronal colonization along the gastrointestinal tract of control and mutant mice, at different stages of early development (E14.5). Whole-mount immunofluorescent staining with the TUJ1 antibody (anti-β3 tubulin) to visualize the neuronal network at E14.5. Schematic representation of the stomach (S.), small intestine (s.i), caecum (ce.) and colon (co.). Lines and perpendicular arrows indicate the extent of gut colonization for each class of genotyped embryos with the number of embryos indicated on the right of each arrow. Enlargements of the terminal region of the colons are visualized in the insert. We noticed an incomplete colonization for mutants compared to control. Double mutant and β1−/− guts are more affected by the colonization process than Ncad−/− guts. Arrows indicate the position of the migratory front in controls and arrowheads indicate the position of the migratory front in mutants. Scale bar = 150 μm.

the 15 experiments performed, we did see round loosely connected clusters of non-adhesive neurons (Fig. 4L, P; white arrowheads) compared with controls (Fig. 4I, M).

We found neurons associated with progenitors and glial cells in all of the cultures. Progenitors and differentiated cells were scattered on the substrata in control, DM, and Ncad-null mutants. In β1-null ENCC, progenitors and glial cells were found in the aggregates in close contact with neurons revealing their inability to adhere to the ECM.

These in vitro results are consistent with the observations of the neuronal network in the whole-mount stained gut. They indicate that the abnormal aggregates formed by β1-null ENCC are mediated by an N-cadherin-dependent mechanism.

Differences in the rostro-caudal organization of the neuronal network in control and mutant guts

We observed rostro-caudal differences in the organization of the neuronal network in E14.5 whole-mount stained guts. This parameter was analyzed in maximum-intensity 3D projections of confocal images of TUJ1 staining (red), YFP-positive ENCC in the myenteric layer (green), and merged images (Fig. 5A). The small intestine and colon were divided into three parts: proximal (Mg1), central (Mg2), and distal small intestine (Mg3); and proximal (Hg1), central (Hg2), and distal colon at the level of the migratory front (Hg3/MF). In the distal colon, the MF localization can vary between controls and mutants. In these zones, ENCC appeared to be present in similar numbers in control and mutant guts. However, a more compact organization of ENCC was observed in the distal small intestine and proximal colon, indicating differences in rostro-caudal organization of ENCC.

We performed quantitative analyses of the ENCC distribution and the neuronal TUJ1$^+$ networks in the guts with different genotypes. The density of ENCC was determined by the quantification of area of spaces devoided of YFP$^+$ (ENCC) (Fig. 5B, S2). The ENCC-free areas of the gut were quantified by K-means segmentation as described in Materials and methods section. Fig. 5B depicts the box-plots illustrating the average area values for each portion of guts for the whole confocal dataset. Each single and double mutant was compared to controls using Student's *t* test. In both controls and mutants, we observed small ENCC-free areas in the Mg2, Mg3, Hg1, Hg2, and Hg3 portions and larger ENCC-free areas in the proximal small intestine (Mg1). Indeed, in the central region of the β1−/− gut (Mg2, Mg3, Hg1, and Hg2 portions), the ENCC-free areas were bigger compared with those of control, Ncad−/−, and DM. The absence of migration of ENCC cells in the Hg3 portions of the β1−/− gut was indicated by higher values of ENCC-free areas. Similarities between control and DM were observed in the Mg portions, suggesting a rescue of

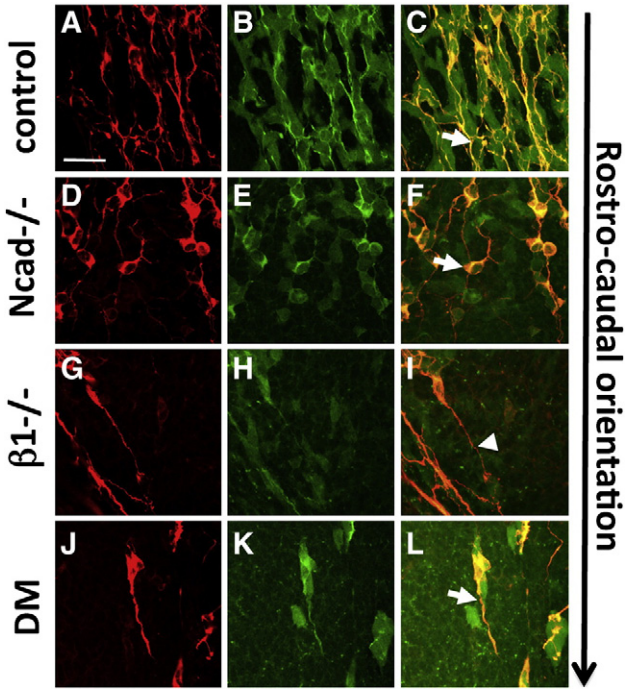

Fig. 3. ENCC distribution (YFP, green) and neuronal network (TUJ1, red) at the wave front of E14.5 hindguts. Control (A, B, C), Ncad−/− (D, E, F), β1−/− (G, H, I), DM (J, K, L). The migratory front (MF) is localized in the Hg3 region for control and Ncad−/− ENCC. The migratory front (MF) is localized in the Hg2 region for β1−/− and DM ENCC due to the delay of migration. The merge is the combination of ENCC (YFP, green) and TUJ1 (red) images. White arrows: neurites associated with ENCC. White arrowheads: neurites not associated with ENCC. Scale bar = 10 μm.

the β1−/− ENCC network organization when N-cadherin was depleted. We checked that the observed differences in the network were due exclusively to changes in distribution rather than the presence of smaller numbers of ENCC. We quantified the total amount of ENCC-free areas, which are expressed as the percentage of the image not containing YFP^+ cells. This gives an estimate of density assuming that single cells have a constant area. The density was not significantly different (Kruskal–Wallis test p-value > 0.05) even when significant differences in total YFP^+-free space were observed. We observed differences in the area of individual ENCC (YFP^+)-free spaces that were not proportional to the difference in the total YFP^+-free area (data not shown). Similar results were obtained at all sites in all conditions, except for the Mg2 region in control and β1−/−, and in DM and β1−/−. In this case, the percentage of the image not covered by YFP^+ cells differed significantly between the control (25 +/− 5%) and β1−/− (45 +/− 5%) but YFP^+-free areas were smaller in the control $(2.4 +/- 0.5).10^4$ pixel squares versus β1−/− $(7.4 +/- 1.1).10^4$ pixel squares. If these differences in YFP^+-free areas resulted purely from the presence of a smaller number of cells, we would expect the same ratio between the average of YFP^+-free space area and the total amount of YFP^+-free areas, but this is not the case. In conclusion, this indicates that the observed differences result from differences in the distribution of equivalent numbers of cells.

We also compared ENS organization in the various conditions by quantifying the texture and performing a principal component analysis (PCA) of the neuronal network ($TUJ1^+$) of control and mutant guts, samples from the same offspring (Figs. 5A, 6), as described in the Materials and methods section. PCA allows either the detection of distinct network organizations whose position in the PCA space is separated by a decision line or ellipse, or similar populations whose dots co-localized. The dots for controls were either co-localized or close to NCad−/− dots in Mg1, Mg2, and Hg1. This indicates that control and Ncad−/− guts have a similar neuronal-network organization. Co-localization of control dots with DM dots was observed in Mg2, Mg3, Hg1, and Hg2 (ellipses), suggesting a rescue of the organization of the DM neuronal network. Furthermore, similarities between control and DM in the network organization before the caecum can be correlated with the organization of ENCC-free spaces (Fig. 5). In contrast, β1−/− dots were separated from the other dots by decision lines in Mg1, Mg3, and Hg2. This demonstrates a distinct organization of neuronal networks in β1−/− throughout the gut compared with control, Ncad−/−, and DM. These differences correlate with the differences in the measurements of ENCC-free spaces in β1−/− (Fig. 5B).

PCA of the Hg3 region did not include β1−/− or DM dots due to the lack of mutant ENCC in this portion of the gut. Analysis of another dataset is shown in supplementary materials (Fig. S3) and gave similar results. For clarity, the two experiments were not compiled in one graph because of variations in the confocal laser settings and variability between different littermates.

This analysis demonstrated that the β1-integrin depletion in ENCC leads to a significant change in the ENS network, with larger ganglia and a larger meshwork size than observed for N-cadherin depletion or the double depletion. The removal of N-cadherin in the β1-null context rescued a normal organization of neuronal network in the DM midgut. Alongside the data from ex vivo cultures, these results indicate that the organization of the ENS network is modulated by interplay between β1-integrins and N-cadherin.

Migration properties of mutant ENCC during hindgut colonization (E12.0–E12.5)

To analyze the dynamics of ENCC behavior, we cultured whole guts and visualized the migration of YFP-positive cells within the gut tissue through time-lapse imaging coupled with fluorescence microscopy. We analyzed both the speed of migration and directionality of movement of ENCC. The directionality of control and mutant ENCC was evaluated by measuring the angle between the rostro-caudal axis of the gut and the straight line separating the initial and final positions of the cell (Fig. 7C, D). The directionality was perturbed in Ncad−/− compared to controls. Control ENCC migrated in the hindgut by forming ramified chains with complex trajectories at the wave front. This migration was often preceded by advanced isolated cells before ENCC finally joined them at the front, as shown in the Supplementary materials section (Fig. S4-A; Movie 1, Supplementary material; Fig. 7A,C). These findings are in agreement with previous observations (Druckenbrod and Epstein, 2007; Young et al., 2004b). In contrast, Ncad−/− ENCC exhibit transient adhesions between each other, with trajectories mostly oriented perpendicularly to the rostro-caudal axis; some cells are also observed migrating caudo-rostrally (Figure S4-B, Movie 2, Supplementary material; Fig. 7B,D). At the migratory front, control and Ncad−/− ENCC exhibited a similar speed of locomotion (30.7 +/− 3 μm/h and 30.5 +/− 1.5 μm/h, respectively; Fig. 7E). These results are consistent with the 35 μm/h speed at which GFP+ cells have been reported to migrate at E12.5 in the hindgut (Young et al., 2004b).

By E12.5, the wave front for β1−/− ENCC was at the caecum, whereas the wave fronts for DM ENCC were at the midgut (Fig. 1). We previously described a severe migratory defect for β1−/− ENCC in the midgut and proximal hindgut (Breau et al., 2009). A similar observation was made for DM ENCC, which exhibited a low speed of locomotion (15 +/− 4 μm/h) and aberrant directionality in the distal midgut (data from Fig.S4-D; Movie 4, Supplementary material). Time-lapse imaging showed a few isolated ENCC localized ahead of the migratory front in both β1−/− and DM (data from Movies 3 and 4, respectively, in Supplementary materials). However, in this gut portion at this stage, these cells were almost static with a speed

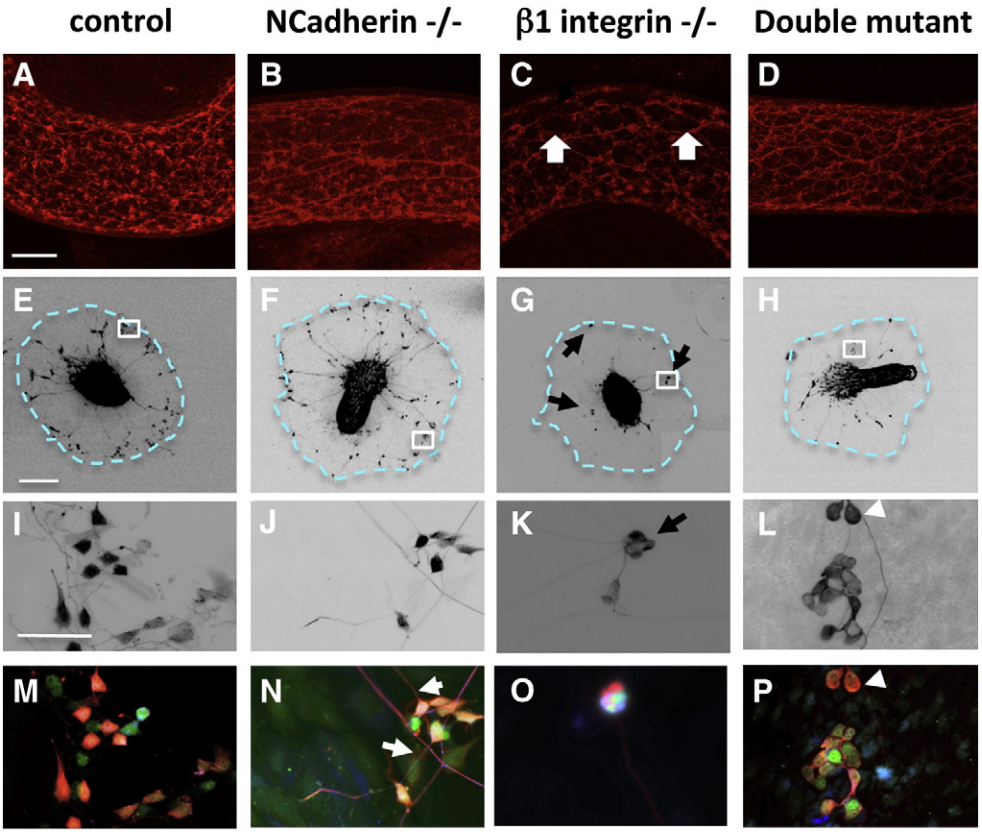

Fig. 4. Neuronal network organization in the midgut of control and mutants. A–D: Confocal compilation of TUJ1 whole-mount immunostaining (x10), Scale bar = 20 μm. Neuronal network organization for control (A), Ncad mutant (B), β1 integrin mutant (C), and double mutant (D). In β1 integrin mutants (C), TUJ1-free spaces (white arrows) and bigger ganglia are observed. A partial rescue of the ganglia network organization is observed in double mutants (D) suggesting that the abnormal aggregation of β1-null ENS network is driven by an N-cadherin dependent mechanism. E–L: Visualization of gut explants cultured in vitro and immunostained with HuD markers labeling neuronal cell bodies, and NF160 markers labeling neuronal processes. E–H: low magnification (×10 objective); Scale bar = 100 μm; blue dashed lines represent the extent of migration of smooth muscle cells migrating out of the explants; ENCC shown in white boxes correspond to the higher magnification images visualized in I–L (×60 objective); Scale bar = 10 μm. At high magnification, spheroid aggregates are only observed in β1mutants (K). M–P: Immunostaining of progenitors (Sox10+), neurons (HuD+), and glial cells (B-FABP+) are visualized respectively in green, red, and blue, in control (M), Ncad−/− (N), β1−/− (O), DM (P) gut cultures. Black arrows indicate ENCC clusters observed in β1−/− mutant guts.

of 1.5 +/− 0.9μm/h. These isolated cells probably originated from ENCC cells migrating laterally from the midgut region through the mesentery. This process was sometimes observed in controls and mutants, where ENCC cross laterally through the mesentery, from the midgut to the hindgut, without migration into the caecum (data from Fig. S4-E; Movie 5, Supplementary material). Similar observations have been previously reported (Enomoto, H and Young, H.M., 2009, at the 2nd International Symposium on Development of the enteric nervous system, London U.K.).

Our results suggest that the transient delay of colonization between controls and Ncad mutants is probably due to a directionality defect of Ncad−/− ENCC. The defect in gut colonization by the DM arises from a combined alteration of the speed and directionality, as observed for β1−/− mutants.

Double N-cadherin and β1-integrin depletion leads to embryonic lethality

We then analyzed the consequences of DM deletion and compared this with β1-integrin and N-cadherin deletion, during embryogenesis and after birth. A total of 781 embryos from 143 matings were examined from E11.5 to E18.0. As shown in Table 1A, in the context of the Ht–PA–Cre/Ht–PA–Cre;$Ncad^{neo/wt}$;$β1^{neo/wt}$ genotype, lower percentages of DM (13%) and Ncad−/− (13%) mutants were obtained, compared with the expected Mendelian rate of 25%. β1−/− genotypes were obtained at the expected percentage (25%), whereas the percentage for controls was higher than expected (49%). Embryo viability was analyzed at each stage (Table 1B). Viability was higher for Ncad−/− and β1−/− than for DM. We also observed that the highest lethality for DM occurs between E10.0 and E11.0.

We also generated crossings to produce newborn Ncad−/− and double mutants. Among the newborn mice obtained (n = 31), we never obtained animals with a DM genotype, indicating that inactivation of both N-cadherin and β1-integrin genes in NCC is embryonically lethal. In contrast, 15 Ncad-mutant mice survived without any detectable abnormalities for at least up to 7 months, whereas 4 β1 mutant mice died within the first 3 weeks after birth (previously described (Breau et al., 2009)). These findings indicate that a synergy between N-cadherin and β-1 integrin during NCC ontogenesis is required for embryonic development.

The Ht–PA–Cre promoter used in our assays targets the ENS and the peripheral nervous system, as well as the other NCC derivatives, including cardiac derivatives (Pietri et al., 2003). Earlier deletion of N-cadherin from NCC using Wnt1–cre caused cardiac outflow tract defects and embryonic lethality (Luo et al., 2006). It would therefore be of interest to analyze the heart and other different organs where NCC play a crucial role in development in DM embryos at various stages of development, to elucidate the cause of lethality before birth.

Impact of the depletion of N-cadherin and β1-integrin on ENCC differentiation

We next determined whether deletion of genes encoding N-cadherin and β1-integrin affected ENCC differentiation. As previously described in

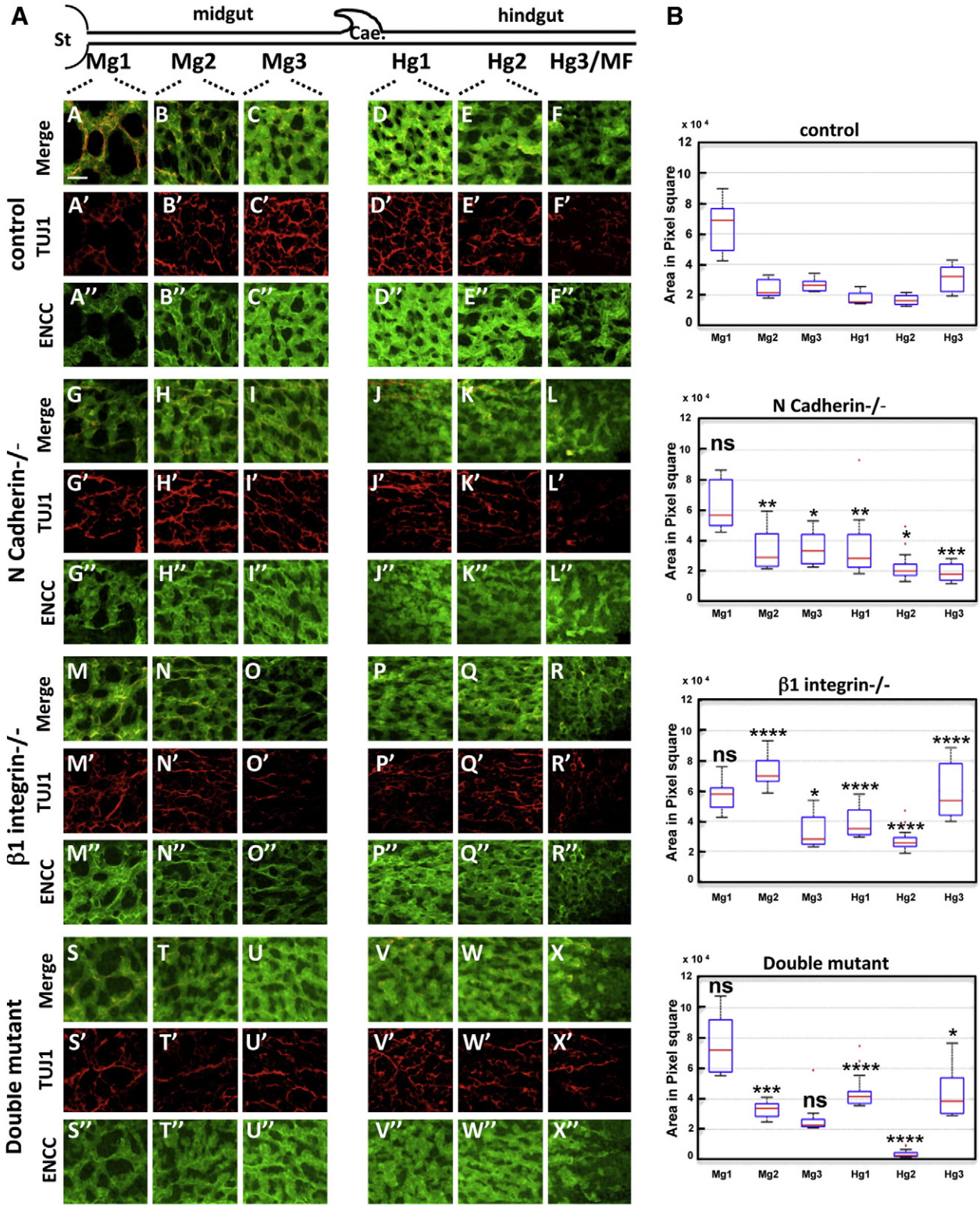

Fig. 5. Quantitative analysis of ENCC distribution and neuronal network organization along the intestinal tract of control and mutant guts (E14.5). A: Schematic representation of the gut along the rostro-caudal axis (stomach, small intestine, caecum, colon). The small intestine and the colon have been each divided into three parts (Mg1, Mg2 and Mg3) and (Hg1, Hg2 and Hg3), respectively. The migratory front (MF) is localized in the Hg3 region for control and Ncad−/− ENCC. For β1−/− and DM ENCC, the MF is localized in the Hg2 region due to the delay in migration. The merge is the combination of ENCC (YFP, green) and TUJ1 (red) images. Scale bar = 15 μm. B: quantification of ENCC-free regions along the gastrointestinal tract, segmented by K-means as described in Materials and methods section. Area measurements of each cell-free region are expressed in pixel squares and are summarized as box plots, where the top and bottom of each box in blue are the 25th and 75th percentiles of the cell-free regions areas, respectively. The red line in the middle is the median of these areas, the black lines show the full interquartile range. The red crosses indicate outliers. Each mutant was independently compared to control by Student's *t* test with *P<0.05, **P<0.01, *** $P<10^{-4}$ and ****$P<10^{-5}$.

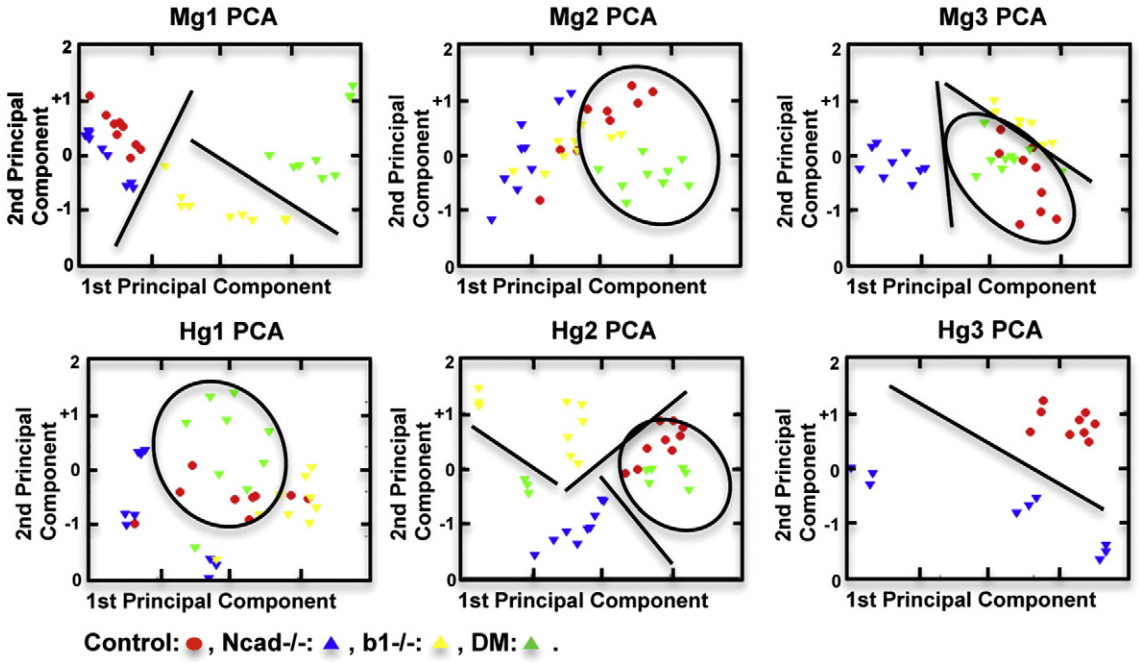

Fig. 6. PCA analysis of the neuronal network of control and mutant mice. We use the GLCM criteria values at an offset of 10. Scatter-plot diagrams in the PCA space of confocal data set for Mg1, Mg2, Mg3, Hg1, Hg2, and Hg3. Control (red dots), N-cad−/− (blue dots), β1−/−(yellow dots) and DM (green dots). The decision black lines or ellipses discriminate between similar or different neuronal network organizations as described in Results section.

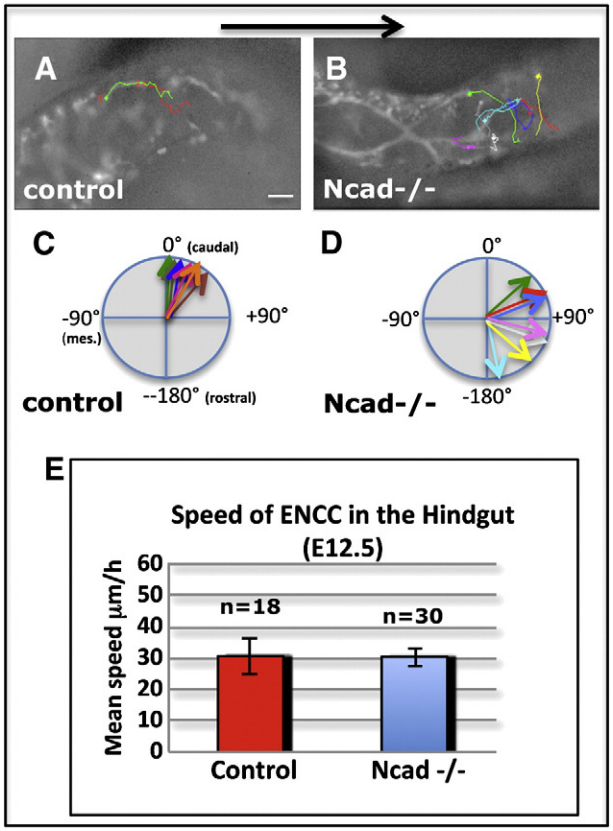

Fig. 7. Time-lapse imaging and tracking of leading YFP$^+$ ENCC in the control and mutant hindguts. ENCC migratory properties within the gut tissue on ex vivo control and Ncad mutant gut cultures. Colored lines show trajectories of tracked ENCC (YFP$^+$): long trajectories are observed for control and Ncad−/− ENCC. Mean directionality of control (C) and N-cad mutant (D) ENCC, evaluated by measuring the angle between the rostro-caudal axis of the gut and the straight line separating the initial and final positions of the cell. For Ncad−/− null ENCC, directionality is altered compared with control. E: Mean speed of leading ENCC; the speed of each cell was calculated by dividing the total length of the trajectory by the time. Error bars indicate s.e.m. Scale bar = 40 µm.

Breau et al. (2009), we performed cell dissociation of control and mutant whole guts and quantified the proportion of progenitors and differentiated cell-specific markers (Fig. 8). Gut dissociations were performed at E13.5 to better identify B-FABP$^+$ glial ENCC because only small numbers of B-FABP$^+$ cells are observed at E11.5 (Young et al., 2003). Cells were counted and identified on the basis of the following criteria: progenitors (Sox10+, Hu−/NF160−, B-FABP−), neurons (Sox10−, Hu+/NF160+, B-FABP−), and glial cells (Sox10+, Hu−/NF160−, B-FABP+). Compared with controls (counted cells, n = 633), progenitors, neurons and glial cells were found in similar proportions in N-cad−/− (n = 263) and β1−/− mutants (n = 494). In contrast, a decrease in the number of progenitors and an increase in the number of glial cells were obtained in DM (n = 425), as shown Fig. 8.

N-cadherin depletion in ENCC does not induce translocation of β-catenin into the nucleus

Loss in cadherin expression affects β-catenin localization and its expression levels in cells, depending on the Wnt signaling status. We examined whether the inactivation of N-cadherin could influence the localization of β-catenin on E12.5 gut sections, when mutant ENCC exhibited delayed migration compared with controls. Sub-localization of β-catenin (Fig. 9, green) was analyzed in ENCC expressing the p75^{NTR} marker for vagal NCC (Fig. 9, red). We observed β-catenin localization at ENCC cell−cell contacts in controls (Fig. 9B white arrow, C) and in β1−/− mutants (Fig. 9H white arrow, I), a shown by the yellow staining in the merge (Fig. 9C and I). In contrast, a very faint signal was detected in Ncad−/− ENCC (Fig. 9E white arrowheads, F) and in DM ENCC (Fig. 9K white arrowheads, L), confirmed by the red staining in the merge (Fig. 9F and L). We observed no nuclear β-catenin staining in control and mutant ENCC, carried out in the appropriate conditions. Intestinal adenoma tissue obtained from Notch/APC mice, was used as a positive control for nuclear β-catenin staining. We detected β-catenin in the cytoplasm and nucleus of tumor cells (Fig. 9M, black arrows) as described by Fre et al. (2009). Beside tumor cells, normal cells (white arrow) displayed membrane β-catenin staining at intercellular adhesions (Fig. 9M, white arrow).

Table 1
Number and percentages of embryos analyzed for each class of genotyped embryos.

A

Genotypes	Embryos E11.0–E18.0	Expected Mendelian rate	Genotypes	Embryos E11.0–E18.0	Expected Mendelian rate	Genotypes	Embryos E11.0–E18.0	Expected Mendelian rate
$Ncad^{fl/fl}$	72/550 (13%)	25%	$Ncad^{fl/fl}$	56/165 (34%)	50%	$\beta1^{l/fl}$	34/66 (52%)	50%
$\beta1^{l/fl}$	140/550 (25%)	25%	control	109/165 (66%)	50%	control	32/66 (48%)	50%
DM	70/550 (13%)	25%						
Control	268/550 (49%)	25%						

B

Stage	Nb#	Control	$Ncad^{fl/fl}$	$\beta1^{l/fl}$	DM
E11.5	91	48/91 (53%)	8/91 (8.8%)	17/91 (18.6%)	8/91 (8.8%)
E12.0–12.5	435	212/435 (48.7%)	78/435 (5.6%)	90/435 (20.7%)	35/435 (8%)
E13.0–E13.5	136	59/136 (43.4%)	25/136 (18.3%)	38/136 (13.2%)	10/136 (7.3%)
E14.0–E14.5	68	28/68 (41.2%)	14/68 (20.5%)	17/68 (25%)	7/68 (10.3%)
E15.0–E18.0	95	45/95 (47.3%)	15/95 (15.8%)	22/95 (23.1%)	10/95 (10.5%)

Discussion

Cell migration is a process that is of major importance during early embryonic development, organ formation, wound-healing, and cancer. Cells migrate either as single cells or in cohorts of interacting cells over long distances and require precise guidance signals to reach their final destination, as reviewed recently in (Friedl and Alexander, 2011). The present study focuses on ENCC that migrate in a rostro-caudal orientated wave, proliferate, encounter various extracellular matrix components, interact with each other, and respond to environmental cues to progress correctly toward the distal gut. ENCC can form chains of migrating cells, associated with neurites (Hao and Young, 2009; Landman et al., 2011). Migration is essential to distribute the ENCC throughout the gut but critical numbers of NCC are required to ensure complete ENS formation (Simpson et al., 2006, 2007). Our data show that cell—cell and cell—matrix adhesion are two required parameters for efficient ENCC migration and proper organization of the ENS. We also provide evidence for a cooperative effect of N-cadherin and β1-integrin during ENS development.

N-cadherin depletion alters ENCC directional migration

Our results demonstrate that the Ncad—/— ENCC migratory front is slightly delayed compared with control ENCC at stage E12.5 of gut development. However, this delay is transient since the location of the ENCC front is similar to that of controls at E14.5 and later stages. However, both intercellular and migratory properties are perturbed in Ncad—/— ENCC since these cells form mostly transient adhesions. As shown in the video data (Supplementary material, Fig. S4B), Ncad—/— ENCC (Movie 2) do not form the characteristic chain-like mode of migration of control cells in the hindgut (Movie 1). Although the speed of ENCC locomotion is unaffected by the N-cadherin mutation, the directionality is impaired. However, these two alterations of mutant-cell migratory behavior did not impede efficient colonization of the gut by stage E14.5-E18.5. This indicates that N-cadherin is not prominent in the control of ENCC progression within the gut wall. Our results are consistent with previous data demonstrating decreased directional movement in Ncad-null ENCC in culture (Xu et al., 2001). However, in contrast with our results, the authors reported an increased migration of Ncad-deficient ENCC, which could be due to differences in vivo versus in vitro conditions.

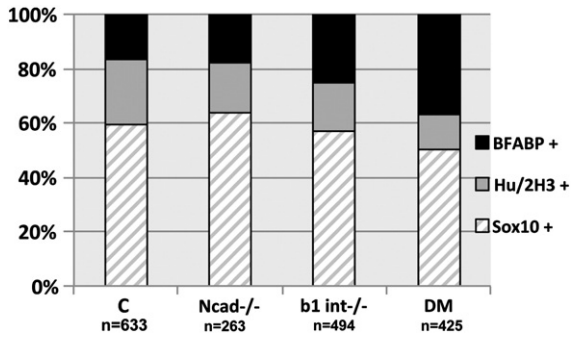

Fig. 8. Percentages of undifferentiated progenitors, neurons and glial cells from dissociated guts at E13.5 plated on vitronectin substrata. Proportions of Sox10+ progenitors (hatched), HuD+ neurons (gray) and B-FABP glial cells (black) are shown in the graph. n=number of ENCC analyzed. C is for controls; β1 int−/− is for β1−/−.

It is well documented that NCC emerge from the neural tube by epithelial—mesenchymal transition (EMT). This process gives NCC the ability to migrate (Kuriyama and Mayor, 2008; Thiery, 2002). The directional migration of group of cells is dependent of cell—cell contact and contact inhibition (Carmona-Fontaine et al., 2008). Until now, there are more examples of the prominent role of N-cadherin in cell migration during chick and *Xenopus* early development than in mice (Detrick et al., 1990; Duband et al., 1988; Hatta et al., 1987; Pla et al., 2001). During development, N-cadherin, Reelin and Rap1 orient the migration of multipolar neurons in the cortex towards the cortical plate (Jossin and Cooper, 2011). N-cadherin also controls directional chain migration of cerebellar granule neurons (Rieger et al., 2009). The altered directionality of Ncad—/— ENCC throughout the gut (Fig. 6B, D) described in the present study is consistent with these observations. This indicates that N-cadherin is required to orient cell migration in both the ENS and the mammalian neocortex. The mechanism by which N-cadherin regulates cell migration is currently unclear. N-cadherin may contribute to transmit traction forces between moving ENCC to promote their collective cell migration as well as a coordinated response to chemoattractants present in the gut wall, such as GDNF or endothelin-3. It would be interesting to dissect the downstream signaling mechanisms of N-cadherin that orient ENCC during the rostro-caudal waves of migration.

Cadherin-6, cadherin-11, NCAM, and L1CAM are other cell-cell adhesion molecules expressed by ENCC (Breau and Dufour, 2009). These adhesion molecules and the integrin repertoire expressed by ENCC are not modified in the Ncad mutant (Broders-Bondon F., unpublished observations), and they may compensate for the lack of N-cadherin function in mutant ENCC. However, germline null mutations in either cadherin-6 or -11 are compatible with embryonic development indicating that neither gene is essential for NCC ontogeny (Jia et al., 2011; Schneider et al., 2012). L1CAM knock-down results in a slight and transient delay of ENCC migration during the early stages of gut development, whereas treatment with anti-L1 blocking antibodies alters the chain-like migration of ENCC (Anderson et al., 2006). It would

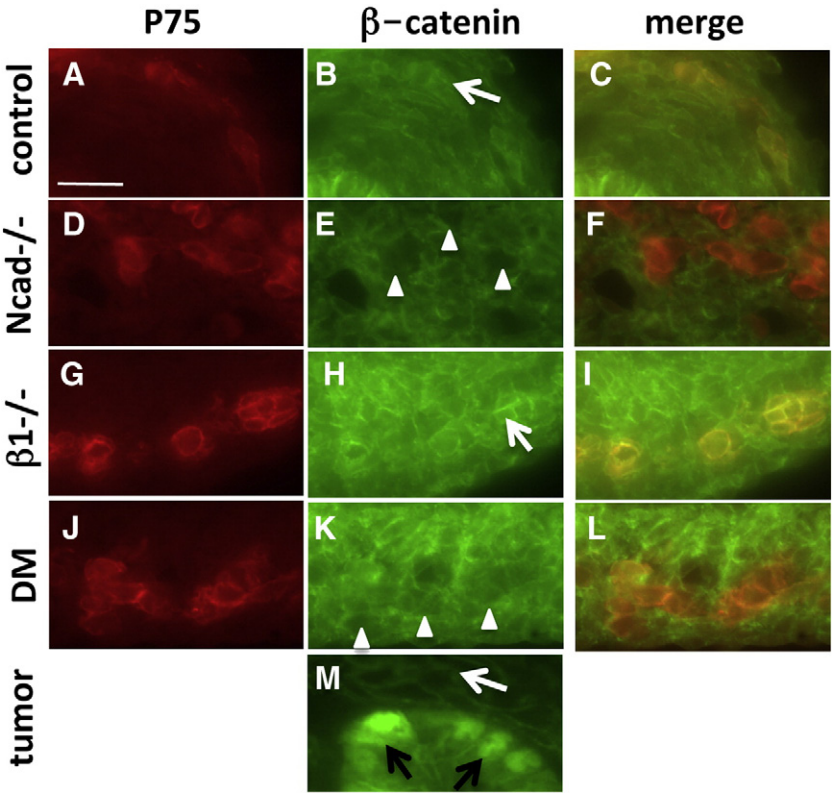

Fig. 9. Membrane localization of β-catenin on sections of control and mutant midguts (A–L). Immunolocalization of β-catenin (green) and P75 (red) on paraffin sections of E12.5 midguts. ENCC or neurons and their precursors are detected in red with $P75^{NTR}$ (A, D, G, J). β-catenin localization is observed at ENCC cell–cell contacts in controls (B white arrow, C) and in β1−/− mutants (Fig. 9H, white arrow; I). A decrease of β-catenin staining is observed in Ncad−/− (E white arrowheads, F) and DM (K white arrowheads, L) compared with control (B, C) and β1−/− (H, I). Nuclear localization of β-catenin is not detected in ENCC. M: tumor cells from intestinal adenoma dissected from Notch/APC mice exhibit β-catenin nuclear staining (black arrow); beside tumor cells, normal cells display β-catenin staining at the membrane (white arrow). Scale bar = 10 μm.

therefore be of interest to test the possible interplay between L1-CAM and N-cadherin in the control of the migratory modes of ENCC during gut development.

N-cadherin and β1-integrin cooperate during gangliogenesis

At different stages of development, the delay of colonization observed in DM is higher than in single mutants and controls, indicating that N-cadherin and β1-integrin cooperate during the migratory process and that N-cadherin mutation enhances the effect of β1-integrin depletion in ENCC. We also report changes in the distribution and the organization of ENCC within the gut tissue that differ between control and single-mutants (Figs. 5 and 6). It is well documented that ENCC progressively differentiate into neurons during their rostro-caudal migration, and extend axons caudally via growth cones (Young et al., 2002). ENCC interactions with axons probably contribute to the organization of the neuronal network.

Axons are usually closely associated with ENCC (Hao and Young, 2009). The present study demonstrates similar findings for controls, Ncad−/− and DM where ENCC at the wave front were associated with axons ($TUJ1^+$ processes), indicating that this process was not under the control of N-cadherin-mediated adhesion or that it could be supported by other intercellular adhesion receptors (see latter in the discussion) in the absence of N-cadherin. By contrast, β1−/− axons were found in advance of the ENCC front, consistent with the notion that their growth is independent of β1-integrins. These findings are consistent with our previous demonstration that neuritogenesis occurs in response to GNDF in β1−/− gut explants embedded in a 3D-collagen environment (Breau et al., 2006). By contrast, our result also provides insight into the roles of the roles of β1 integrins and cell−matrix adhesions during the ENCC migration.

The axon projections ahead of the ENCC migratory front were not observed in the DM (Fig. 3), indicating that this process is controlled by a fine balance between cell−cell and cell−matrix interactions and co-operation between N-cadherin and β1 integrins. Indeed, axons could use N-cadherin as a favorable substrate or as a migratory stimulus (Viollet and Doherty, 1997). This receptor has been shown to contribute to the mechanical coupling with the cell cytoskeleton via catenins (Thoumine et al., 2006), a process supporting axonal growth. We showed that the β1−/− ENCC formed a larger number of intercellular adhesions and larger aggregates. This phenomenon was rescued in the DM, indicating that it resulted from an increase in N-cadherin-mediated adhesion in β1−/− ENCC. The change in the balance between cell−cell and cell−matrix adhesion and its consequences in mutants shed light on the mechanisms governing ENCC migration, in vivo, and highlight the critical role of adhesion balance in the advance of cells in the gut wall and on the axonal growth.

N-cadherin, N-CAM and L1 are three CAMs that play important roles as axonal growth promoting cues, via the FGF receptor. Our results are also consistent with the requirement for additional adhesion molecules in the control of axonal growth when N-cadherin is depleted.

Changes in apoptosis and proliferation have been associated with colonization defects of the gut (Simpson et al., 2007; Uesaka et al., 2008). However, we did not detect any changes in ENCC density in single mutants, double mutants, and controls. $YFP+/TUJ1^+$ ENCC appeared to be present at a normal density in the small intestine and the colonized part of the colon (Fig. 5). In contrast, the double mutants had a reduced percentage of progenitor cells and an increased percentage of glial derivatives at E13.5. It is well known that stem cells are present among migrating NCC and that stem cells express high levels of β1 integrins (Prowse et al., 2010). Our

results indicate that loss of N-cadherin together with β1-integrin would increase progenitor differentiation toward the glial-cell lineage. Nevertheless, the mechanisms by which N-cadherin and β1-integrin co-depletion lead to more glial differentiation are currently unknown. However, cell dissociation was performed on whole-guts but it would be possible that changes in the rate of differentiation occurs only at the colonization front and in that case would not be detected by analyzing dissociated cells from the whole gut. Interestingly, mice with Hand2 deletion in the Nestin-expressing population exhibit abnormal proportion of neuron and glial cell numbers (Lei and Howard, 2011), indicating that specification and expression of neurotransmitters are regulated by Hand2. Because N-CAM is a Hand-2 target (Holler et al., 2010), we could speculate that any modification of ENCC adhesive properties could also affect cell specification.

N-cadherin depletion rescues the neuronal network organization of β1 mutants

Our data show that the elimination of N-cadherin rescues the neuronal organization and distribution of β1−/− ENCC. We propose a model to account for this, based on the assumption that cells always tend to optimize their adhesion to the environment. In Ncad−/−, there is a reduction of cell–cell adhesion due to loss of N-cadherin. This modifies the balance between cell–cell and cell–ECM adhesions in favor of cell adhesion to ECM, which then predominates, favoring the spreading of cells on the ECM. Conversely, in β1−/− ENCC, adhesion to the ECM is weaker due to the loss of β1-integrins. This changes the overall adhesion balance in favor of the intercellular adhesion, which then predominates. This is consistent with the findings of previous studies showing that the disruption of integrin-mediated adhesion in NCC increases N-cadherin mediated adhesion (Monier-Gavelle and Duband, 1997). The increase in intercellular adhesion stimulates ENCC aggregation and neurite fasciculation and modifies the overall organization of the neuronal network. In double mutants, the simultaneous decreases in intercellular adhesions due to the loss of N-cadherin and in cell–ECM adhesions, due to the depletion of β1-integrins, restores the balance between the two types of adhesions although DM ENCC display lower overall levels of adhesion than controls. This leads to normal ENCC aggregation and neurite fasciculation. However, the rescued ENS network organization is not associated with a rescue of migration mode. The overall level of adhesion in the DM is therefore insufficient to result in efficient migration. As DM ENCC display slower colonization than single mutants, we could speculate that N-cadherin and β1-integrins both contribute to the advance of ENCC in the developing gut and that the lower levels of colonization observed in the β1−/− mutant are not only due to the exacerbated intercellular adhesion of ENCC.

ENCC migration does not require Wnt/ catenin signaling

The function of cadherin in cell motility may be separate from its role in cell adhesion. It has been reported that the β-catenin-binding domain of N-cadherin is not required for axonal outgrowth (Riehl et al., 1996), and that cell motility is instead modulated by p120 (Chauvet et al., 2003). Changes in cadherin expression affect β-catenin expression in the absence of Wnt-dependent signaling. Our results show no β-catenin at the membrane of Ncad−/− and DM ENCC and the faint or undetectable signal in the cytoplasm suggest that β-catenin undergoes proteasomal degradation via the axin/APC/GSK3 complex. Alternatively, the β-catenin in Ncad−/− and DM ENCC may be less stable after fixation and treatment before labeling (MacDonald et al., 2009). No nuclear localization of β-catenin was detected in control or mutant ENCC (Fig. 9), indicating that β-catenin does not accumulate in the nuclei and does not transactivate Wnt/β-catenin-dependent genes. Our results are consistent with those for cardiac NCC (Xu et al., 2001), where a marked reduction in cell-surface expression of β-catenin in N-cadherin-deficient NCC was observed. The authors also analyzed the effects of Wnt1 knock-out on NCC migration and found no significant effect on NCC motility (Xu et al., 2001). In conjunction with these findings for cardiac NCC, our data suggest that Wnt/β-catenin signaling is not involved in ENCC migration in the gut during early stages of development. In Xenopus, it has been reported that contact inhibition of locomotion controls NCC directional migration by a non-canonical Wnt signaling mechanism (Carmona-Fontaine et al., 2008). These results suggest that cell–cell contact polarizes NCC, by regulating the accumulation of elements of the PCP signaling pathway. In further studies, it would be interesting to determine whether the PCP pathway is involved in ENCC migration.

Conclusions

Many publications now support the existence of crosstalk between cadherins and integrins in the control of cellular behavior (de Rooij et al., 2005; Gimond et al., 1999; Huttenlocher and Horwitz, 2011; Marsden and DeSimone, 2003; Quadri, 2012; Yano et al., 2004). Some of these studies analyzed this crosstalk using biophysical approaches at the single-cell scale, on micropatterned surfaces, on microarrays of force sensors, or by laser tweezers (Al-Kilani et al., 2011; Borghi et al., 2010; Ganz et al., 2006; Martinez-Rico et al., 2010). These studies indicate that this crosstalk has either a positive or negative effect on cell adhesion, depending on the cellular and environmental context.

It has been previously shown that β1-integrin depletion in ENCC severely affects ENS organization by increasing cell aggregation through a calcium-dependent mechanism involving cadherins (Breau et al., 2006). In the present study, we showed that N-cadherin and β1-integrin molecules both cooperate to efficiently populate the gastrointestinal tract and the ganglia network organization. These findings highlight the complex regulation that exists between cell–cell and cell–matrix adhesion molecules during ENS ontogenesis, reveal that the correct balance between these two types of adhesion processes is crucial for ENS ontogenesis and point out that the collective ENCC migration requires enough levels of both cell–cell and cell–ECM adhesion and thus the finely tuned expression of both N-cadherin and β1-integrin.

Supplementary data associated with this article can be found, in the online version, at doi:10.1016/j.ydbio.2012.02.001.

Acknowledgments

This work was supported by the Centre National de la Recherche Scientifique, the Institut Curie and the Association pour la Recherche sur le Cancer (ARC) (Grant 4864). The anti-NF160 mAb (2H3) was obtained from Developmental Studies Hybridoma Bank, developed under the auspices of the NICHD and maintained by the Department of Biological Sciences, University of Iowa, Iowa City, IA 52242. We thank T. Müller and R.M Mège for providing us with anti-B-FABP and anti cadherin-6 antibodies, respectively, and S. Fre and S. Robine for adenoma intestinal tumor paraffin sections. We thank N. Bondurand for advices and reading of the manuscript. We thank L. Sengmanivong from the NIMCE@Institut Curie-CNRS, V. Fraisier et F. Waharte from the PICT-IBiSA@Lhomond for their help with imaging on video and confocal microscopy; S. Mahieux, L. Raban, A. Dahmani, J. Ripa and J. Heysch for their successive technical assistance; I. Grandjean, S. Jannet and S. Boissel from the Mice Facility-Institut Curie.

References

Al-Kilani, A., de Freitas, O., Dufour, S., Gallet, F., 2011. Negative feedback from integrins to cadherins: a micromechanical study. Biophys. J. 101, 336–344.

Amiel, J., Sproat-Emison, E., Garcia-Barcelo, M., Lantieri, F., Burzynski, G., Borrego, S., Pelet, A., Arnold, S., Miao, X., Griseri, P., Brooks, A.S., Antinolo, G., de Pontual, L., Clement-Ziza, M., Munnich, A., Kashuk, C., West, K., Wong, K.K., Lyonnet, S., Chakravarti, A., Tam, P.K., Ceccherini, I., Hofstra, R.M., Fernandez, R., 2008.

Hirschsprung disease, associated syndromes and genetics: a review. J. Med. Genet. 45, 1–14.
Anderson, R.B., Turner, K.N., Nikonenko, A.G., Hemperly, J., Schachner, M., Young, H.M., 2006. The cell adhesion molecule L1 is required for chain migration of neural crest cells in the developing mouse gut. Gastroenterology 130, 1221–1232.
Barlow, A.J., Wallace, A.S., Thapar, N., Burns, A.J., 2008. Critical numbers of neural crest cells are required in the pathways from the neural tube to the foregut to ensure complete enteric nervous system formation. Development 135, 1681–1691.
Borghi, N., Lowndes, M., Maruthamuthu, V., Gardel, M.L., Nelson, W.J., 2010. Regulation of cell motile behavior by crosstalk between cadherin- and integrin-mediated adhesions. Proc. Natl. Acad. Sci. U. S. A. 107, 13324–13329.
Breau, M.A., Dufour, S., 2009. Biological development of the enteric nervous system. Hirschsprung's Disease: Diagnosis and Treatment. Nova, New York.
Breau, M.A., Pietri, T., Eder, O., Blanche, M., Brakebusch, C., Fassler, R., Thiery, J.P., Dufour, S., 2006. Lack of beta1 integrins in enteric neural crest cells leads to a Hirschsprung-like phenotype. Development 133, 1725–1734.
Breau, M.A., Dahmani, A., Broders-Bondon, F., Thiery, J.P., Dufour, S., 2009. Beta1 integrins are required for the invasion of the caecum and proximal hindgut by enteric neural crest cells. Development 136, 2791–2801.
Bronner-Fraser, M., Artinger, M., Muschler, J., Horwitz, A.F., 1992. Developmentally regulated expression of a6 integrin in avian embryos. Development 115, 197–211.
Campbell, I.D., Humphries, M.J., 2011. Integrin structure, activation, and interactions. Cold Spring Harb. Perspect. Biol. 3.
Carmona-Fontaine, C., Matthews, H.K., Kuriyama, S., Moreno, M., Dunn, G.A., Parsons, M., Stern, C.D., Mayor, R., 2008. Contact inhibition of locomotion in vivo controls neural crest directional migration. Nature 456, 957–961.
Chauvet, N., Prieto, M., Fabre, C., Noren, N.K., Privat, A., 2003. Distribution of p120 catenin during rat brain development: potential role in regulation of cadherin-mediated adhesion and actin cytoskeleton organization. Mol. Cell. Neurosci. 22, 467–486.
de Rooij, J., Kerstens, A., Danuser, G., Schwartz, M.A., Waterman-Storer, C.M., 2005. Integrin-dependent actomyosin contraction regulates epithelial cell scattering. J. Cell Biol. 171, 153–164.
Detrick, R.J., Dickey, D., Kintner, C.R., 1990. The effects of N-cadherin misexpression on morphogenesis in *Xenopus* embryos. Neuron 4, 493–506.
Dima, A.A., Elliott, J.T., Filliben, J.J., Halter, M., Peskin, A., Bernal, J., Kociolek, M., Brady, M.C., Tang, H.C., Plant, A.L., 2011. Comparison of segmentation algorithms for fluorescence microscopy images of cells. Cytometry A 79, 545–559.
Druckenbrod, N.R., Epstein, M.L., 2005. The pattern of neural crest advance in the cecum and colon☆. Dev. Biol. 287, 125–133.
Druckenbrod, N.R., Epstein, M.L., 2007. Behavior of enteric neural crest-derived cells varies with respect to the migratory wavefront. Dev. Dyn. 236, 84–92.
Duband, J.-L., Volberg, T., Sabanay, I., Thiery, J.P., Geiger, B., 1988. Spatial and temporal distribution of the adherens-junction-associated adhesion molecule A-CAM during avian embryogenesis. Development 103, 325–344.
Faure, C., Chalazonitis, A., Rheaume, C., Bouchard, G., Sampathkumar, S.G., Yarema, K.J., Gershon, M.D., 2007. Gangliogenesis in the enteric nervous system: roles of the polysialylation of the neural cell adhesion molecule and its regulation by bone morphogenetic protein-4. Dev. Dyn. 236, 44–59.
Fre, S., Pallavi, S.K., Huyghe, M., Lae, M., Janssen, K.P., Robine, S., Artavanis-Tsakonas, S., Louvard, D., 2009. Notch and Wnt signals cooperatively control cell proliferation and tumorigenesis in the intestine. Proc. Natl. Acad. Sci. U. S. A. 106, 6309–6314.
Friedl, P., Alexander, S., 2011. Cancer invasion and the microenvironment: plasticity and reciprocity. Cell 147, 992–1009.
Gaidar, Y.A., Lepekhin, E.A., Sheichetova, G.A., Witt, M., 1998. Distribution of N-cadherin and NCAM in neurons and endocrine cells of the human embryonic and fetal gastroenteropancreatic system. Acta Histochem. 100, 83–97.
Ganz, A., Lambert, M., Saez, A., Silberzan, P., Buguin, A., Mege, R.M., Ladoux, B., 2006. Traction forces exerted through N-cadherin contacts. Biol. Cell 98, 721–730.
Gimond, C., van Der Flier, A., van Delft, S., Brakebusch, C., Kuikman, I., Collard, J.G., Fassler, R., Sonnenberg, A., 1999. Induction of cell scattering by expression of beta1 integrins in beta1-deficient epithelial cells requires activation of members of the rho family of GTPases and downregulation of cadherin and catenin function. J. Cell Biol. 147, 1325–1340.
Gumbiner, B.M., 2005. Regulation of cadherin-mediated adhesion in morphogenesis. Nat. Rev. Mol. Cell Biol. 6, 622–634.
Hao, M.M., Young, H.M., 2009. Development of enteric neuron diversity. J. Cell. Mol. Med. 13, 1193–1210.
Hatta, K., Takagi, S., Fujisawa, H., Takeichi, M., 1987. Spatial and temporal expression pattern of N-cadherin cell adhesion molecules correlates with morphogenetic proccesses of chicken development. Dev. Biol. 120, 215–227.
Heanue, T.A., Pachnis, V., 2007. Enteric nervous system development and Hirschsprung's disease: advances in genetic and stem cell studies. Nat. Rev. Neurosci. 8, 466–479.
Holler, K.L., Hendershot, T.J., Troy, S.E., Vincentz, J.W., Firulli, A.B., Howard, M.J., 2010. Targeted deletion of Hand2 in cardiac neural crest-derived cells influences cardiac gene expression and outflow tract development. Dev. Biol. 341, 291–304.
Huttenlocher, A., Horwitz, A.R., 2011. Integrins in cell migration. Cold Spring Harb. Perspect. Biol. 3.
Hynes, R.O., 2002. Integrins: bidirectional, allosteric signaling machines. Cell 110, 673–687.
Iwashita, T., Kruger, G.M., Pardal, R., Kiel, M.J., Morrison, S.J., 2003. Hirschsprung disease is linked to defects in neural crest stem cell function. Science 301, 972–976.
Jia, L., Liu, F., Hansen, S.H., Ter Beest, M.B., Zegers, M.M., 2011. Distinct roles of cadherin-6 and E-cadherin in tubulogenesis and lumen formation. Mol. Biol. Cell 22, 2031–2041.
Jiang, Q., Ho, Y.Y., Hao, L., Nichols Berrios, C., Chakravarti, A., 2011. Copy number variants in candidate genes are genetic modifiers of Hirschsprung disease. PLoS One 6, e21219.
Jossin, Y., Cooper, J.A., 2011. Reelin, Rap1 and N-cadherin orient the migration of multipolar neurons in the developing neocortex. Nat. Neurosci. 14, 697–703.
Kasemeier-Kulesa, J.C., Bradley, R., Pasquale, E.B., Lefcort, F., Kulesa, P.M., 2006. Eph/ephrins and N-cadherin coordinate to control the pattern of sympathetic ganglia. Development 133, 4839–4847.
Kostetskii, I., Li, J., Xiong, Y., Zhou, R., Ferrari, V.A., Patel, V.V., Molkentin, J.D., Radice, G.L., 2005. Induced deletion of the N-cadherin gene in the heart leads to dissolution of the intercalated disc structure. Circ. Res. 96, 346–354.
Kruger, G.M., Mosher, J.T., Tsai, Y.H., Yeager, K.J., Iwashita, T., Gariepy, C.E., Morrison, S.J., 2003. Temporally distinct requirements for endothelin receptor B in the generation and migration of gut neural crest stem cells. Neuron 40, 917–929.
Kuriyama, S., Mayor, R., 2008. Molecular analysis of neural crest migration. Philos. Trans. R. Soc. Lond. B Biol. Sci. 363, 1349–1362.
Landman, K.A., Fernando, A.E., Zhang, D., Newgreen, D.F., 2011. Building stable chains with motile agents: insights into the morphology of enteric neural crest cell migration. J. Theor. Biol. 276, 250–268.
Lei, J., Howard, M.J., 2011. Targeted deletion of Hand2 in enteric neural precursor cells affects its functions in neurogenesis, neurotransmitter specification and gangliogenesis, causing functional aganglionosis. Development 138, 4789–4800.
Luo, Y., High, F.A., Epstein, J.A., Radice, G.L., 2006. N-cadherin is required for neural crest remodeling of the cardiac outflow tract. Dev. Biol. 299, 517–528.
MacDonald, B.T., Tamai, K., He, X., 2009. Wnt/beta-catenin signaling: components, mechanisms, and diseases. Dev. Cell 17, 9–26.
Marsden, M., DeSimone, D.W., 2003. Integrin-ECM interactions regulate cadherin-dependent cell adhesion and are required for convergent extension in *Xenopus*. Curr. Biol. 13, 1182–1191.
Martinez-Rico, C., Pincet, F., Thiery, J.P., Dufour, S., 2010. Integrins stimulate E-cadherin-mediated intercellular adhesion by regulating Src-kinase activation and actomyosin contractility. J. Cell Sci. 123, 712–722.
Monier-Gavelle, F., Duband, J., 1997. Cross talk between adhesion molecules: control of N-cadherin activity by intracellular signals elicited by beta1 and beta3 integrins in migrating neural crest cells. J. Cell Biol. 137, 1663–1681.
Muldoon, T.J., Thekkek, N., Roblyer, D., Maru, D., Harpaz, N., Potack, J., Anandasabapathy, S., Richards-Kortum, R., 2010. Evaluation of quantitative image analysis criteria for the high-resolution microendoscopic detection of neoplasia in Barrett's esophagus. J. Biomed. Opt. 15, 026027.
Nakagawa, S., Takeichi, M., 1998. Neural crest emigration from the neural tube depends on regulated cadherin expression. Development 125, 2963–2971.
Parisi, M.A., Kapur, R.P., 2000. Genetics of Hirschsprung disease. Curr. Opin. Pediatr. 12, 610–617.
Pietri, T., Eder, O., Blanche, M., Thiery, J.P., Dufour, S., 2003. The human tissue plasminogen activator-Cre mouse: a new tool for targeting specifically neural crest cells and their derivatives in vivo. Dev. Biol. 259, 176–187.
Pietri, T., Eder, O., Breau, M.A., Topilko, P., Blanche, M., Brakebusch, C., Fässler, R., Thiery, J.P., Dufour, S., 2004. Conditional 1-integrin gene deletion in neural crest cells causes severe developmental alterations of the peripheral nervous system. Development 131, 3871–3883.
Pla, P., Moore, R., Morali, O.G., Grille, S., Martinozzi, S., Delmas, V., Larue, L., 2001. Cadherins in neural crest cell development and transformation. J. Cell. Physiol. 189, 121–132.
Potocnik, A.J., Brakebusch, C., Fassler, R., 2000. Fetal and adult hematopoietic stem cells require beta1 integrin function for colonizing fetal liver, spleen, and bone marrow. Immunity 12, 653–663.
Prowse, A.B., Chong, F., Gray, P.P., Munro, T.P., 2010. Stem cell integrins: implications for ex-vivo culture and cellular therapies. Stem Cell Res. 6, 1–12.
Quadri, S.K., 2012. Cross talk between focal adhesion kinase and cadherins: role in regulating endothelial barrier function. Microvasc. Res. 83, 3–11.
Radice, G.L., Rayburn, H., Matsunami, H., Knudsen, K.A., Takeichi, M., Hynes, R.O., 1997. Developmental defects in mouse embryos lacking N-cadherin. Dev. Biol. 181, 64–78.
Rieger, S., Senghaas, N., Walch, A., Koster, R.W., 2009. Cadherin-2 controls directional chain migration of cerebellar granule neurons. PLoS Biol. 7, e1000240.
Riehl, R., Johnson, K., Bradley, R., Grunwald, G.B., Cornel, E., Lilienbaum, A., Holt, C.E., 1996. Cadherin function is required for axon outgrowth in retinal ganglion cells in vivo. Neuron 17, 837–848.
Schneider, D.J., Wu, M., Le, T.T., Cho, S.H., Brenner, M.B., Blackburn, M.R., Agarwal, S.K., 2012. Cadherin-11 contributes to pulmonary fibrosis: potential role in TGF-{beta} production and epithelial to mesenchymal transition. FASEB J. 26, 503–512.
Simpson, M.J., Landman, K.A., Hughes, B.D., Newgreen, D.F., 2006. Looking inside an invasion wave of cells using continuum models: proliferation is the key. J. Theor. Biol. 243, 343–360.
Simpson, M.J., Zhang, D.C., Mariani, M., Landman, K.A., Newgreen, D.F., 2007. Cell proliferation drives neural crest cell invasion of the intestine. Dev. Biol. 302, 553–568.
Srinivas, S., Watanabe, T., Lin, C.S., William, C.M., Tanabe, Y., Jessell, T.M., Costantini, F., 2001. Cre reporter strains produced by targeted insertion of EYFP and ECFP into the ROSA26 locus. BMC Dev. Biol. 1, 4.
Stanchina, L., Baral, V., Robert, F., Pingault, V., Lemort, N., Pachnis, V., Goossens, M., Bondurand, N., 2006. Interactions between Sox10, Edn3 and Ednrb during enteric nervous system and melanocyte development. Dev. Biol. 295, 232–249.
Thiery, J.P., 2002. Epithelial–mesenchymal transitions in tumour progression. Nat. Rev. Cancer 2, 442–454.
Thoumine, O., Lambert, M., Mege, R.M., Choquet, D., 2006. Regulation of N-cadherin dynamics at neuronal contacts by ligand binding and cytoskeletal coupling. Mol. Biol. Cell 17, 862–875.
Uesaka, T., Nagashimada, M., Yonemura, S., Enomoto, H., 2008. Diminished Ret expression compromises neuronal survival in the colon and causes intestinal aganglionosis in mice. J. Clin. Invest. 118, 1890–1898.

Viollet, C., Doherty, P., 1997. CAMs and the FGF receptor: an interacting role in axonal growth. Cell Tissue Res. 290, 451–455.
Wallace, A.S., Schmidt, C., Schachner, M., Wegner, M., Anderson, R.B., 2010. L1cam acts as a modifier gene during enteric nervous system development. Neurobiol. Dis. 40, 622–633.
Xu, X., Li, W.E., Huang, G.Y., Meyer, R., Chen, T., Luo, Y., Thomas, M.P., Radice, G.L., Lo, C.W., 2001. Modulation of mouse neural crest cell motility by N-cadherin and connexin 43 gap junctions. J. Cell Biol. 154, 217–230.
Yano, H., Mazaki, Y., Kurokawa, K., Hanks, S.K., Matsuda, M., Sabe, H., 2004. Roles played by a subset of integrin signaling molecules in cadherin-based cell–cell adhesion. J. Cell Biol. 166, 283–295.
Young, H.M., Jones, B.R., McKeown, S.J., 2002. The projections of early enteric neurons are influenced by the direction of neural crest cell migration. J. Neurosci. 22, 6005–6018.
Young, H.M., Bergner, A.J., Müller, T., 2003. Acquisition of neuronal and glial markers by neural crest-derived cells in the mouse intestine. J. Comp. Neurol. 456, 1–11.
Young, H., Anderson, R., Anderson, C., 2004a. Guidance cues involved in the development of the peripheral autonomic nervous system. Auton. Neurosci. 112, 1–14.
Young, H.M., Bergner, A.J., Anderson, R.B., Enomoto, H., Milbrandt, J., Newgreen, D.F., Whitington, P.M., 2004b. Dynamics of neural crest-derived cell migration in the embryonic mouse gut. Dev. Biol. 270, 455–473.